Trim Analysis of Helicopter Rotor in Forward Flight

Xingda Cui, Lu Zhang, Weibin Li, Shuai Ma, Junfeng Sun, Zhongyun Xiao *

Computational Aerodynamics Institute, China Aerodynamics Research and Development Center, Mianyang 621000, China

* Corresponding Author Email: scxiaozy@sina.cn

Abstract. Rotor trim is an important prerequisite for conducting an accurate aerodynamic computation of helicopter rotor. In order to accurately obtain the rotor control settings such as collective pitch and cyclic pitch, trim analysis of helicopter rotor in forward flight based on CFD method is carried out. Firstly, a rotor trimming method for forward flight and CFD numerical method are introduced. Then, the moving-embedded grid method is applied to perform trim calculation on the flowfield of AH-1G rotor under forward flight test condition. Finally, the CFD calculation of rotor control settings are compared with flight test data. The comparison results suggest that the rotor trimming and CFD numerical methods are reasonable and feasible for the numerical simulation on unsteady flowfield of a trimmed rotor in forward flight. Compared with flight test data, the calculated collective pitch of trimmed AH-G rotor is about 0.19 degrees smaller with an error of 3.2%. The calculated rotor control settings have a certain degree of accuracy, which can meet the engineering application needs on evaluation of trimmed helicopter rotor control settings and lay the foundation for further accurate numerical simulation research of rotor aerodynamic characteristics.

Keywords: Enter key words or phrases in alphabetical order, separated by commas.

1. Introduction

Unlike the steady flow around fixed wing aircraft, the helicopter rotor flow is a typical unsteady flow. Even in the steady forward flight state, there exists the wide variation of the incoming flow velocity and local angle of attack of the rotor blade around the azimuth due to the rotation of the rotor and the twist of the blade [1]. Due to the variation of Mach number along the blade span, the flowfield of rotor has both the incompressible flow region at the blade root and the sub-transonic flow region at the blade tip [2]. The rotor wake and the tip vortices generated at the tips of the rotating blades further lead to a complex flowfield of helicopter rotor such as interactions between the rotating blades and vortex, interactions between fuselage and vortex and so on [3-6]. So, it is difficult to simulate the flowfield around a helicopter rotor accurately [7-10]. For a long time, the design of helicopter rotor mainly depends on various simplified theories for aerodynamic performance analysis, and then continuously revised and improved according to the ground or wind tunnel tests.

With the development of numerical methods and high-performance computer technology, modern computational fluid dynamics (CFD) method has not only been widely applied in predicting the aerodynamic performance of fixed-wing aircraft [11-12], but also made significant progress in simulating the unsteady flowfield of helicopter rotors [13-15]. The main advantage of the CFD method by solving the Reynolds-averaged Navier-Stokes equations is that it can capture and transfer vorticity in the computational domain without making the assumption of irrotational, and make vorticity exist as a part of the equation solution. Due to the consideration of the viscosity of the gas, the Navier-Stokes equations can accurately describe the formation and transport of vortices. Under the framework of the Navier-Stokes equations, the details of the complex flowfield can be studied in more depth, such as interactions between blades and wake vortex, the blade stall and so on [2]. However, in forward flight helicopter rotor blades accompany periodic motions such as pitch, flapping and swaying. Accurate CFD analysis of helicopter rotors in forward flight requires rotor trim to obtain the collective pitch, cyclic pitch and flapping. The trimming problem [16-17] has become an important factor restricting the further application of CFD method in the simulation of helicopter rotors. Most existing CFD methods of helicopter rotors rely on experimental or comprehensive analysis methods to determine the pitch settings of the blades and the flapping deflections in advance, and then evaluate the aerodynamic characteristics of helicopter rotors. The numerical simulation of the flowfield of forward-flying rotors does not consider rotor trim as part of the solution which has significant limitations for the CFD analysis of rotors. Over the last 20 years, several researchers [17-20] have carried out research on helicopter rotor trim technology combined with CFD method.

Under the support of Chinese national numerical windtunnel project [21], China Aerodynamics Research and Development Center has developed a numerical simulation software named HeliX to simulate the flowfield of hovering and forward-flying rotors. HeliX is the CFD software developed based on structured grid and block structured Cartesian grid, which has the ability of unsteady dynamic grid calculation in the inertial coordinate system, coupled with rotor trim calculation, and can simulate periodic blade motions such as pitch, flapping and swaying.

In this paper, forward flight simulation of a trimmed rotor including the periodic motion of the blades has been undertaken by using HeliX software. Firstly, a rotor trimming method for forward flight and CFD numerical method are introduced. Then, the moving-embedded grid method is applied to perform trim calculation on the flowfield of AH-1G rotor under forward flight test condition. Finally, the CFD calculation of rotor control settings such as the collective pitch and cyclic pitch is compared with flight test data.

2. Rotor Trimming Method

In this paper, the present trimming method neglects the lead-lag defection of the blades. In steady wording condition of forward flight, the pitch and flapping motions of helicopter rotor blades are periodic [17, 19], which can be described as a function of azimuth (ψ):

$$\begin{aligned} \theta &= \theta_0 + \theta_{1c}\cos\psi + \theta_{1s}\sin\psi \\ \beta &= \beta_0 + \beta_{1c}\cos\psi + \beta_{1s}\sin\psi \end{aligned} \tag{1}$$

Where θ and β represent the blade pitch and flapping angles. θ_0 is the collective pitch which is measured at 0.75 of the rotor radius R. β_0 is the coning angle. θ_{1c} and θ_{1s} are the cyclic harmonics. β_{1c} and β_{1s} are the fapping harmonics.

The so-called rotor trimming is to adjusting the rotor control settings of Equation (1) to ensure that the thrust and aerodynamic moments of the rotor are matched to desired target values [20]. In this paper, the collective pitch and cyclic pitch (θ_0, θ_{1c}, θ_{1s}) are the rotor control setting, and the thrust and moment coefficients (C_T, C_{mx}, C_{my}) are the target parameters. The expressions for rotor trimming are defined as

$$\begin{Bmatrix} C_T \\ C_{mx} \\ C_{my} \end{Bmatrix}^{(d)} = \begin{Bmatrix} C_T \\ C_{mx} \\ C_{my} \end{Bmatrix}^{(0)} + J \begin{Bmatrix} \Delta\theta_0 \\ \Delta\theta_{1c} \\ \Delta\theta_{1s} \end{Bmatrix}^{(0)} \tag{2}$$

Where C_{mx} and C_{my} represent the rolling and pitching moment coefficients of the rotor. $C_T{}^{(d)}$ is the target thrust coefficient given in the calculation. The following assumptions are generally made:

$$C_{mx}{}^{(d)} = 0 \tag{3}$$

$$C_{my}{}^{(d)} = 0 \tag{4}$$

The coefficient matrix J before the changes of the control settings $(\Delta\theta_0, \Delta\theta_{1c}, \Delta\theta_{1s})$ is the Jacobian matrix defined as (θ_0, θ_{1c}, θ_{1s})

$$J=\begin{bmatrix}\frac{\partial C_T}{\partial\theta_0} & \frac{\partial C_T}{\partial\theta_{1c}} & \frac{\partial C_T}{\partial\theta_{1s}}\\ \frac{\partial C_{mx}}{\partial\theta_0} & \frac{\partial C_{mx}}{\partial\theta_{1c}} & \frac{\partial C_{mx}}{\partial\theta_{1s}}\\ \frac{\partial C_{my}}{\partial\theta_0} & \frac{\partial C_{my}}{\partial\theta_{1c}} & \frac{\partial C_{my}}{\partial\theta_{1s}}\end{bmatrix} \tag{5}$$

The calculation of each partial derivative in the Jacobian matrix adopts the small perturbation assumptions which are

$$\frac{\partial C_T}{\partial\theta_0}\approx\frac{\Delta C_T}{\Delta\theta_0},\quad \frac{\partial C_{mx}}{\partial\theta_{1c}}\approx\frac{\Delta C_{mx}}{\Delta\theta_{1c}},\quad \frac{\partial C_{my}}{\partial\theta_{1s}}\approx\frac{\Delta C_{my}}{\Delta\theta_{1s}} \tag{6}$$

After one trim cycle, the control settings of the rotor are updated using the following relation:

$$\begin{Bmatrix}\theta_0\\ \theta_{1c}\\ \theta_{1s}\end{Bmatrix}^{(n+1)}=\begin{Bmatrix}\theta_0\\ \theta_{1c}\\ \theta_{1s}\end{Bmatrix}^{(n)}+\begin{Bmatrix}\Delta\theta_0\\ \Delta\theta_{1c}\\ \Delta\theta_{1s}\end{Bmatrix} \tag{7}$$

Where n represent the number of the trim cycle. To obtain the convergence of the trimming procedure, a Newton-Raphson iterative method is used to trim the rotor. A constant trim state is reached when one of the two following convergence conditions is met:

$$\Delta C_T\le\varepsilon_1,\quad \Delta C_{\text{mx}}\le\varepsilon_2,\quad \Delta C_{\text{my}}\le\varepsilon_3 \tag{8}$$

or

$$\Delta\theta_0\le\varepsilon_4,\quad \Delta\theta_{1c}\le\varepsilon_5,\quad \Delta\theta_{1s}\le\varepsilon_6 \tag{9}$$

It should be noted that calculating the Jacobian matrix by CFD method is a time-consuming operation that requires small perturbation computations for the collective pitch and cyclic pitch, and at least ($3/N_b$) revolutions need to be calculated, where N_b represents the number of blades in a rotor. In HeliX software, a simplified strategy is adopted, which assumes that the Jacobian matrix remains unchanged, that is to say, the Jacobian matrix is only calculated in the first trim cycle, and the Jacobian matrix required in subsequent re-trimming is equal to the value obtained from the first trim cycle.

3. Numerical Method

The flow control equations are compressible Navier-Stokes [19] equations described by arbitrary Lagrangian Eluerian formulation, which allows arbitrary movement and deformation of the mesh. The integral forms in absolute coordinate system are expressed as:

$$\frac{d}{dt}\iiint_{\Omega}Qd\Omega+\oiint_{S}(\vec{H}^{I}-Q\vec{V}_{\Omega})\bullet\vec{n}dS=\oiint_{S}\vec{H}^{V}\bullet\vec{n}dS \tag{10}$$

In formula (10), Ω represents the volume of the control body, S represents the area of the boundary interface of the control body, $\vec{V}_{\Omega}$ is the mesh velocity on the boundary interface, and Q is a conserved state variable. $Q=\{\rho,\rho u,\rho v,\rho w,e\}^T$. ρ and e represent the density and total energy of the fluid respectively. $\rho u,\rho v,\rho w$ represent momentum components of the fluid. $\vec{H}^{I}$ is the convective flux on the boundary of the control body, and $\vec{H}^{V}$ is the viscous flux.

Flux difference dispersion based on Roe scheme is used for the convection flux, and the third order accuracy form of Vanalbada limiter is used for MUSCL interpolation. The viscous flux is discretized by using central difference scheme. For the time-accurate simulation, the dual-time stepping with the LU-SGS implicit method is applied to advance the solution in time. The calculation assumes that the flowfield is full turbulence. The turbulence model is k- ω SST two-equation model. In order to accelerate the convergence speed of unsteady flow computations, Multigrid technology is applied [22].

4. Computational Model and Grid

The helicopter rotor simulated in this paper is an AH-1G rotor in forward flight which has rich flight test data in forward flight states [23] and is widely used for the validation of rotorcraft CFD solver [19]. The accuracy and reliability of HeliX software for rotor trimming calculation method can be evaluated by comparing the CFD trimming calculation results of AH-1G rotor with flight test data. AH-1G rotor is a two-bladed rectangular-planform teetering rotor shown in Figure 1. The blade profile is a single OLS aerofoil. The blade has a linear twist of -10 degrees from root to tip. The rotor is a right-handed rotor. The rotor radius R is about 6.7 meters, and the chord length of the rotor blade is about 0.727 meters. The rotor speed is 324rev/min.

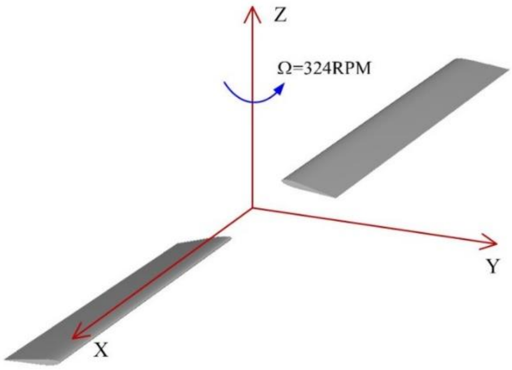

Figure 1. AH-1G rotor model

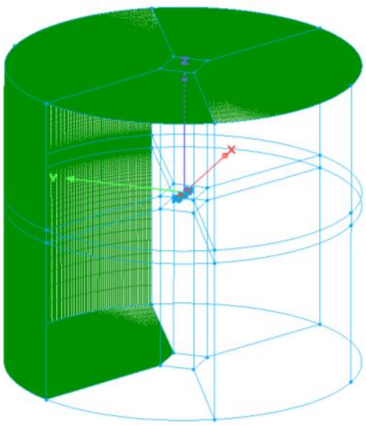

(a) The background grid

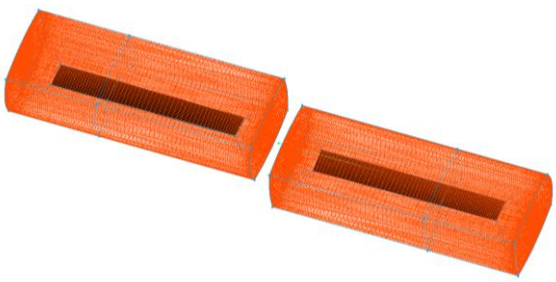

(b)The two subgrids of blades

Figure 2. Computational grid of AH-1G rotor

The difficulty of simulating the rotor flowfield is partly attributed to the simulation of blade motions. The overlap grid methodology is considered one of the most effective methods suiting to solve the problem of moving objects with large displacement among the various developed grid technologies. By using overlap grid methodology, the limitation of multiblock and patched grid is overcome, and the difficulty of generating block-structured grids is reduced. Based on the above considerations, a structured overlap grid methodology is applied to generate a computational grid of AH-1G rotor shown in Figure 2. Computational grid of AH-1G rotor for simulation of the unsteady forward flight state consists of a background grid shown in Figure 2(a) and two block-structured, rigidly-moving subgrids of the blades shown in Figure 2(b). The blade-fixed subgrids are embedded in the background grid. In the background, the distance from the upper boundary to the rotor disk plane is 9R, and the distance from the lower boundary to the rotor disk plane is 11R, the distance from the circumferential boundary to the blade tip is 11R. In order to capture the blade tip vortex accurately and reduce the numerical dissipation, the grids on the distribution area of the blade tip vortex are clustered in the background grid shown in Figure 3. After local grid refinement, the number of grid cells in the background grid has reached over 29 million. For AH-1G rotor blades, O-type topology grids around the blades are constructed to ensure good grid orthogonality at the blade ends. To capture the tip vortex the blade-fixed subgrids are clustered near the leading edges, trailing edges, blade root region and blade tip region. The spacing of the first grid point from the surface of the blade is 0.005mm. The number of grid cells in the two blade subgrids is approximately 3.5 million.

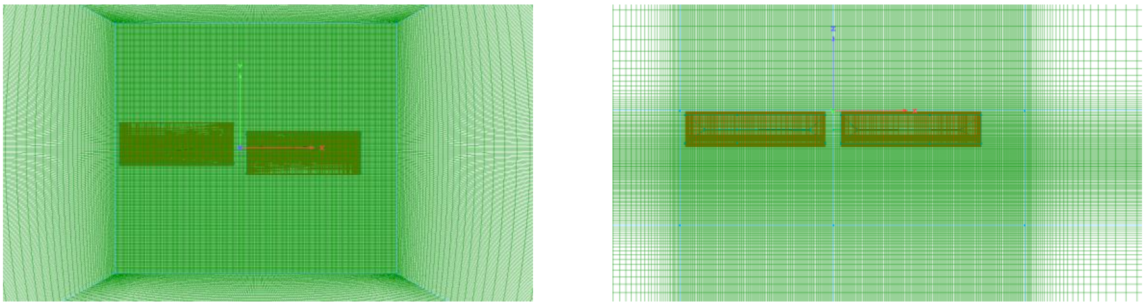

(a) Vertical view (b) Side view

Figure 3. Local grid refinement in the background grid of the AH-1G rotor

Figure 4 shows the overlapped region between the profile grid of the blade subgrid at 0.75*R* and the profile grid of the local background grid. It can be seen that there are more than 4 overlap grid layers between the blade subgrid and the background grid, indicating that the background grid is made reasonably with high quality, and ensure the accuracy of data interpolation and transmission during the subgrids motion.

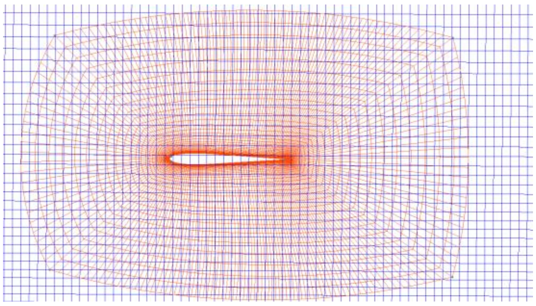

Figure 4. Overlapped grid region

5. Overlap Grid Parallel Assembly

In the calculation of helicopter rotor in forward flight, as using overlap grids to generate calculation grids, multiple subgrids need to be generated for multiple rotor blades, and the number of the total grid cells can easily reach tens of millions or even billions. While overlap grid methodology needs auxiliary algorithm to interchange information between grids [19]. Therefore, it is difficult to meet the actual calculation needs by optimizing grid digging, point finding algorithms and using serial processing methods. For the computational grid of rotor in forward flight, an overlap grid parallel assembly technology [24] is applied in this paper to improve the calculation efficiency of flowfield. On the basis of implementing a single process fast query algorithm, complete parallelization of Chimera grid excavation and interpolation relationship establishment is achieved. The specific process of searching and interpolation relationships can be described as follows: for any interpolation point, first search for the contribution unit at this node, and if not found, send the information of the interpolation point to the other nodes. These nodes simultaneously search for the contribution unit of the interpolation point. If found, return the information of the contribution unit and establish a message transmission relationship between the two nodes. The biggest advantage of this approach is the removal of the so-called root node, which means that the Chimera grid calculation of any node does not need to collect global grid information, reducing the memory requirements of a single node, and avoiding the situation where a single node calculates Chimera interpolation relationships and other nodes wait, improving the assembly efficiency of large-scale overlap grids.

6. Simulation Results and Analysis

In this paper, the flight condition chosen for AH-1G has an advance ratio 0.19, blade tip Mach number of 0.65, a Reynolds number of 9.73×10^6 and a thrust coefficient equal to 0.00464. the convergence criteria for trimming calculation are: the target thrust coefficient is 0.00464, the rolling and pitching moment coefficients are 0. The iteration in the azimuthal direction is 360 per revolution, which corresponds to the azimuth angle increment of 1°. The flapping motion of rotor blade is not simulated during trimming procedure in the present work. The precone and shaft tilt angles are set to zero during the computation. The purpose is to maintain parameter settings consistency between this paper and Reference [19].

Before starting rotor trimming calculation, it is necessary to input the initial control settings of the trim state to initiate unsteady CFD calculations of the rotor. The initial collective pitch of the rotor is generally estimated through empirical formulations or approximate equations [17, 19] based on blade-element theory for the aero-mechanics of the rotor. The initial cyclic pitch is usually set to 0. The initial collective pitch of the rotor given in Reference [20] is adopted in the present work, which is 5.33°. With the initial control settings, a relative steady flow simulation is performed, and periodic variation in rotor thrust, pitching and rolling moment coefficients can be obtained by initial CFD calculations with a certain number of steps (720 steps in the present work). At this time, a prescribed level of convergence is reached basically. Then, the first trim cycle include calculation of the Jacobian matrix is carried out. In this paper, the first trim cycle consists of 2 revolutions of the rotor blade: 1.5 revolutions for calculation of the Jacobian matrix and the rest for solution iteration. As the initial trim is completed, a number of subsequent re-trimming are performed after every 180 iterations in the present work.

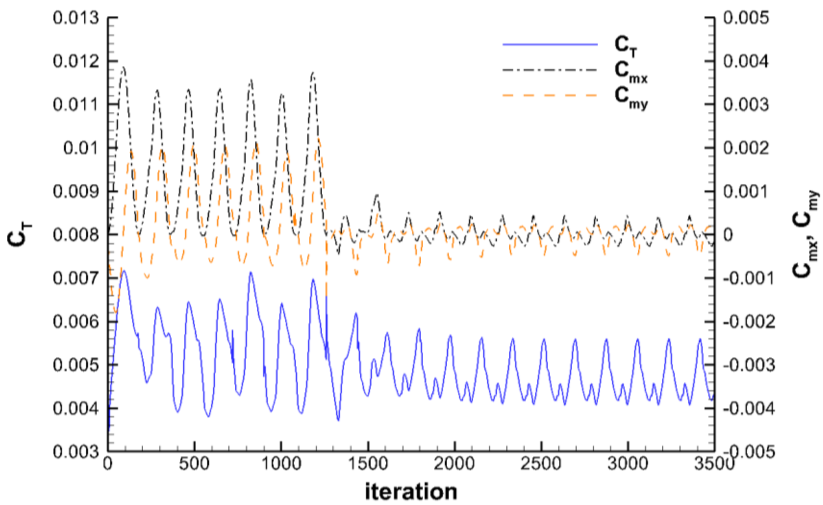

Figure 5. Simulation of forward flight trim-state for AH-1G rotor

Figure 5 shows sample results of instantaneous thrust and moments coefficients obtained from the CFD calculation coupling with the trimming procedure for the AH-1G rotor in forward flight. Figure 5 presents the process with initial 720 iterations which is known as the starting stage of rotor CFD calculation. The starting stage of rotor CFD calculation needs the initial control settings (θ_0 is 5.33°, θ_c and θ_s are 0° in the present work) as input. Figure 6 shows the history of revolution-averaged thrust and moment coefficients of the AH-1G rotor during the trim procedure. It can be seen that the thrust and moment coefficients converge to the desired target value after 6 trim cycles, the CFD simulation presents an oscillatory variation shown in Figure 5. It should be noted that only first trim cycle consists of 2 revolutions while other trim cycle consists of half revolution in the present work. Figure 7 shows the history of control settings of the forward-flying AH-1G rotor during the trim procedure. After the initial trimming and subsequent re-trimmings the solutions of control settings (θ_0, θ_{1c}, θ_{1s}) gradually converge to some fixed values.

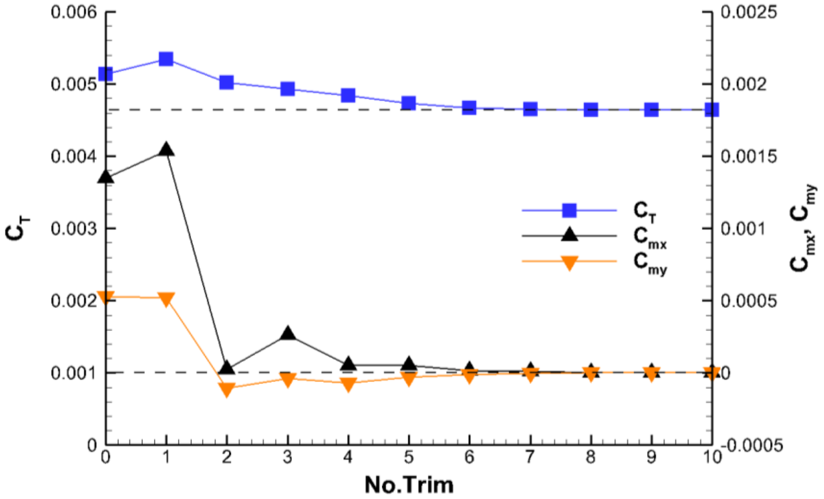

Figure 6. History of revolution-averaged thrust and moment coefficients of AH-1G rotor

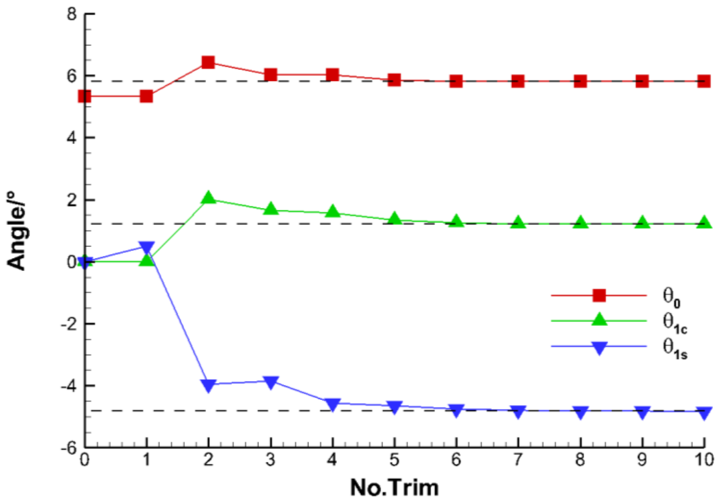

Figure 7. History of control settings of AH-1G rotor in forward flight

Table 1 shows comparison between the trimmed rotor control settings calculated in this paper and flight test data for the AH-1G rotor in forward flight. It can be seen that compared with flight test data [23], the calculated collective pitch θ_0 of trimmed AH-G rotor is about 0.19 degrees smaller, with an error of 3.2%. The difference between the calculated value and experimental data about horizontal cyclic pitch θ_{1c} is about 0.49 degrees, with an error of 28.9%. The difference between the calculated value and experimental data about vertical cyclic pitch θ_{1s} is about 0.67 degrees, with an error of 12.2%. Obviously, the difference between the calculated value of cyclic pitch and the experimental data is relatively larger and could not be ignored. It is believed that the discrepancy may be caused by the aero-elastic effects and interactions between rotor and fuselage. The complex flow phenomena of helicopter such as interactions between the rotating blades and vortex, interactions between rotor and fuselage, aero-elastic effects and so on occurs in the actual flight test. However, the blade elastic deformations and the influence of the fuselage are not considered in the present computations. A similar discrepancy in cyclic pitch for AH-1G rotor is seen in previous literature such as References

[19, 20] without elastic effect in the computations as well. The result of collective pitch computation shows a closer agreement to flight test data than that of cyclic pitch computation. As can be seen, HeliX software has computational accuracy to some extent in the prediction capability of the trimmed rotor control settings, and is able to meet the engineering application needs on evaluation of trimmed helicopter rotor control settings.

Table 1. Comparison of trimmed control settings for AH-1G rotor(degrees)

Data Source	θ_0	θ_{1c}	θ_{1s}
Experiment	6.0	1.7	-5.5
Reference [19]	6.1	1.3	-5.1
Reference [20]	6.1	1.4	-4.9
Present Work	5.81	1.21	-4.83

Table 1 also provides the computed control settings by using the direct CFD trimming method in Reference [19] and the differential CFD trimming method in Reference [20]. Although the blade elastic deformations and the influence of the fuselage are not considered in computations of present work and References [19, 20], the minor discrepancy about computed control settings between the present work and References [19, 20] is still seen. This discrepancy may be caused by differences in the CFD solvers, trimming methods and calculated blade shapes. The CFD solver in the present study and Reference [20] selects the Navier-Stokes equations for simulation, while Reference [19] uses the Euler equations. At the same time, the calculation model simulated in the present study is obtained by stretching a two-dimensional OLS aerofoil into a three-dimensional blade according to the information provided by References [19, 20]. Therefore, there may be some differences in the calculated blade shapes.

Figure 8 shows the computed vorticity contour around AH-1G rotor in forward flight at M_{tip}=0.65 and target C_T=0.00464. The vorticity contour is expressed by Q value which is used to distinguish the three-dimensional flow vortices of fluid [25-26]. It can be seen that the following blade would be affected by the tip vortices generated at previous blade tips during the rotor motions. It demonstrates that the numerical calculation method adopted by HeliX software in this paper has a high accuracy in capturing tip vortex, and can effectively simulate the complex flowfield of helicopter rotor in forward flight.

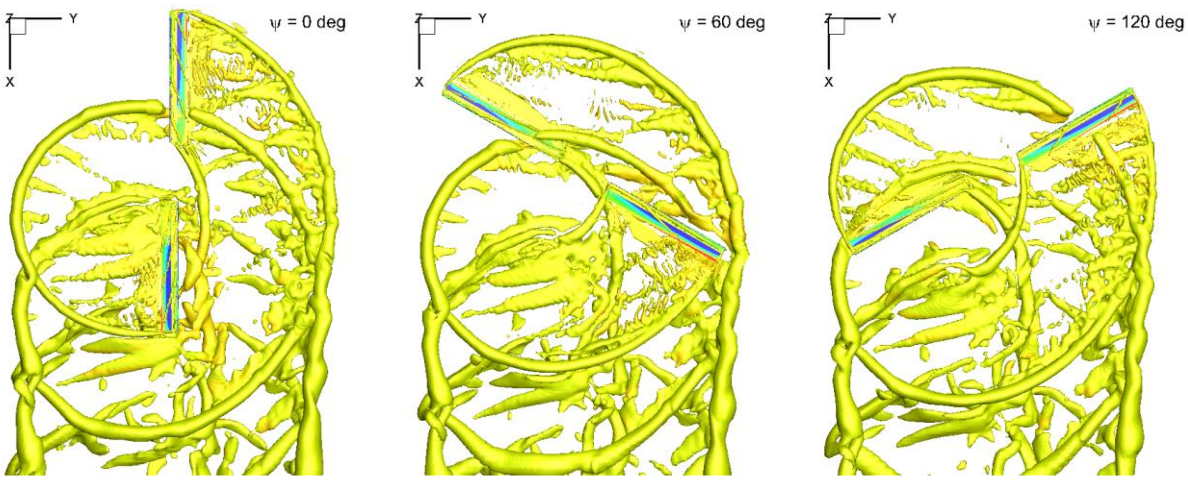

(a) Ψ = 0 deg (b) Ψ = 60 deg (c) Ψ = 120 deg

Figure 8. Computed vorticity contour around AH-1G rotor in forward flight

7. Conclusion

Rotor trim is an important prerequisite for conducting an accurate aerodynamic computation of helicopter rotor. In order to accurately obtain the rotor control settings such as collective pitch and cyclic pitch, trim analysis of helicopter rotor in forward flight based on CFD method is carried out by using HeliX software which is developed independently. Firstly, a rotor trimming method for forward flight and CFD numerical method are introduced. Then, the moving-embedded grid method is applied to perform trim calculation on the flowfield of AH-1G rotor under forward flight test condition. Finally, the CFD calculation of rotor control settings are compared with flight test data. Compared with flight test data, the calculated collective pitch of trimmed AH-G rotor is about 0.19 degrees smaller with an error of 3.2%. The difference between the calculated value and experimental data about horizontal cyclic pitch is about 0.49 degrees, with an error of 28.9%. The difference between the calculated value and experimental data about vertical cyclic pitch is about 0.67 degrees, with an error of 12.2%. Obviously, the agreement with the experiment data is good for the collective pitch. It can be seen that the rotor trimming and CFD numerical methods adopted by HeliX software are reasonable and feasible for the numerical simulation on unsteady flowfield of a trimmed rotor in forward flight. The moving-embedded grid method coupling with an overlap grid parallel assembly technology is suitable for large-scale parallel computation of unsteady forward-flying flowfield of helicopter rotors. It also indicates that HeliX software has computational accuracy to some extent in the prediction capability of the trimmed rotor control settings, and is able to meet the engineering application needs on evaluation of trimmed helicopter rotor control settings. As well, HeliX software has good capture accuracy for tip vortex in forward flight, and can effectively simulate the complex flowfield of helicopter rotor in forward flight. It should be noted that the discrepancy between the calculated values of trimmed rotor control settings in this paper and experimental data, as well as those in References [19, 20], may be related to the factors such as the lack of consideration of rotor aero-elastic effects, interactions between the rotating blades and fuselage, differences in trimming methods, difference in CFD solvers, and differences in calculated blade shapes for the computations. In order to improve prediction capability, additional investigations with more accurate comparison between the computed control settings and experimental data in forward flight will be carried out by considering the blade elastic deformations, improving the trimming method, and adopting a consistent rotor-fuselage model.

References

[1] S.C. Wang, G.H. Xu, Progress of Helicopter Rotor Aerodynamics, Journal of Nanjing University of Aeronautics & Astronautics, 2001, 33(3): 203-211.

[2] Z.Y. Xiao, Investigation of Computational Modeling Techniques for Rotor Flowfields, China Aerodynamic Research and Development Center, Mianyang, 2007.

[3] W. Johnson, Rotorcraft aeromechanics, Cambridge university press, 2013.

[4] G.H. Xu, Q.J. Zhao, Z. Gao, et al, Prediction of aerodynamic interactions of helicopter rotor on its fuselage, Chinese Journal of Aeronautics, 2002, 15(1): 12-17.

[5] X. Jiang, Z.Y. Xiao, Z.B. Chen, et al. Numerical simulation of Rotor/Airframe Aerodynamic Interaction, Helicopter Technique, 2007, 151(3): 4-10.

[6] J.G. Leishman, N. Bi, Aerodynamic interactions between a rotor and a fuselage in forward flight, Journal of the American Helicopter Society, 1990, 35(3): 22-31.

[7] Y.M. Park, O.J. Kwon. Simulation of Unsteady Rotor Flow Using Unstructured Adaptive Sliding Meshes, Journal of the American Helicopter Society, 2004, 49(4):391-400.

[8] H. Pomin, S. Wagner. Navier-Stokes Analysis of Helicopter Rotor Aerodynamics in Hover and Forward Flight, Journal of Aircraft, 2002, 39(5):813-821.

[9] H. Pomin, S. Wagner. Aeroelastic analysis of helicopter rotor blades on deformable chimera grids. Journal of Aircraft, 2004, 41(3):577–584.

[10] R. Renzoni, A.D. Alascio, N. Kroll, et al. A common European Euler code for the analysis of the helicopter rotor flowfeld. Progress in Aerospace Sciences, 2000, 36:437– 485.

[11] Z. Zhou, J. T. Huang, Y. Huang, et al. CFD technology in aeronautic engineering field: Applications, challenges and development. Acta Aeronautica et Astronautica Sinica, 2017, 38(3): 1-25.

[12] C. Yan. Achievements and predicaments of CFD in aeronautics in past forty years. Acta Aeronautica et Astronautica Sinica, 2022, 43(10): 21-57.

[13] G.H. Xu, Q.J. Zhao, Advances in CFD of helicopter rotor, Journal of Nanjing University of Aeronautics & Astronautics, 2003, 35(3): 338-344.

[14] R.C. Strawn, F.X. Carodonna, E.P.N. Duque, 30 years of rotorcraft computational fluid dynamics research and development, Journal of the American Helicopter Society, 2006, 51(1): 5-20.

[15] Z.Y. Xiao, Y.H. Guo, L. Zhang, et al. An analysis of current status and prospects of CFD based simulation of rotorcrafts. Acta Aerodynamica Sinica, 2021, 39(4):14-25.

[16] A.T. Conlisk. Modern helicopter aerodynamics. Annual Review of Fluid Mechanics,1997, 29:515-567.

[17] R. Steijl, G. Barakos and K. Badcock. A framework for CFD analysis of helicopter rotors in hover and forward flight. International Journal for Numerical Methods in Fluids, 2006, 51:819–847.

[18] K. Chung, C. Hwang, Y. Park, et al. Numerical predictions of rotorcraft unsteady air-loadings and BVI noise by using a time-marching free-wake and acoustic analogy. 31th European Rotorcraft Forum, Firenz, 2005.

[19] J. W. Kim, S. H. Park, and Y. H. Yu. Euler and Navier-Stokes simulations of helicopter rotor blade in forward flight using an overlapped grid solver. 19th AIAA Computational Fluid Dynamics, San Antonio, Texas, 22-25 June 2009.

[20] Z. Ye, Y. J. Shi, G. H. Xu.Analytical method of rotor aerodynamic characteristics by coupling a high-efficiency trim strategy. Journal of Aerospace Power, 2017, 32(4):882-889.

[21] J.Q. Chen, Advances in the key technologies of Chinese national numerical windtunnel project, SCIENTIA SINICA Technologica, 2021, 51(11): 1326-1347.

[22] B. Mou, Z.Y. Xiao, Z. Zhou, et al, Application and investigation of multiblock multigrid method in complicated viscous flow fields calculation, Acta Aerodynamica Sinica, 2006, 24(1): 51-54.

[23] J.L. Cross, M.E. Watts. Tip aerodynamics and acoustics test: a report ad data survey. NASA-RP-1179, 1988.

[24] Y. H. Guo, X. Jiang, Z. Y. Xiao, et al. An automatic parallel and implicit assembly method for overset grid. Acta Aeronautica et Astronautica Sinica, 2021, 42(6): 312-330.

[25] Z. Li, X.W. Zhang, F. He, Evaluation of vortex criteria by virtue of the quadruple decomposition of velocity gradient tensor, Acta Physica Sinica, 2014, 63(5): 1-7.

[26] T.F. Egeberg, Onset and progressing of vortical structures for a surface combatant at drift angles 0, 10 and 20 degrees, Norwegian University of Science and Technology, Trondheim, 2013.